Anal Bioanal Chem (2008) 391:1759–1772
DOI 10.1007/s00216-008-2045-5

ORIGINAL PAPER

# Electrically detected displacement assay (EDDA): a practical approach to nucleic acid testing in clinical or medical diagnosis

**P. Liepold · T. Kratzmüller · N. Persike · M. Bandilla · M. Hinz · H. Wieder · H. Hillebrandt · E. Ferrer · G. Hartwich**

Received: 6 December 2007 / Revised: 26 February 2008 / Accepted: 29 February 2008 / Published online: 20 April 2008


**Abstract** This paper introduces the electrically detected displacement assay (EDDA), a electrical biosensor detection principle for applications in medical and clinical diagnosis, and compares the method to currently available microarray technologies in this field. The sensor can be integrated into automated systems of routine diagnosis, but may also be used as a sensor that is directly applied to the polymerase chain reaction (PCR) reaction vessel to detect unlabeled target amplicons within a few minutes. Major aspects of sensor assembly like immobilization procedure, accessibility of the capture probes, and prevention from nonspecific target adsorption, that are a prerequisite for a robust and reliable performance of the sensor, are demonstrated. Additionally, exemplary results from a human papillomavirus assay are presented.

P. Liepold · T. Kratzmüller · N. Persike · M. Bandilla · M. Hinz · H. Wieder · H. Hillebrandt · E. Ferrer · G. Hartwich (✉)
FRIZ Biochem Gesellschaft für Bioanalytik mbH,
82061 Neuried, Germany
e-mail: Gerhard.Hartwich@frizbiochem.de
URL: www.frizbiochem.de

H. Wieder
Roche Diagnostics GmbH,
Sandhofer Str. 116,
68305 Mannheim, Germany

H. Hillebrandt
Roche Diagnostics GmbH,
Nonnenwwlad 2,
82377 Penzberg, Germany

E. Ferrer
Kendle GmbH + Co.GMI KG,
Stefan-George-Ring 6,
81929 München, Germany

**Keywords** Microarray · Electrical detection · Biosensor · HPV · Genotyping

**Abbreviations**

| | |
|---|---|
| ACV | alternating current voltammetry |
| CP | capture probe |
| CPG | controlled pore glass |
| CV | cyclic voltammetry |
| DBU | diazabicycloundecene |
| DMAP | 4-dimethylaminopyridine |
| DMF | dimethylformamide |
| DMSO | dimethylsulfoxide |
| ds | double stranded |
| DTE | dithioerythritol |
| DTPA | dithiolphosphoamidite |
| EC | electrochemical |
| EDDA | electrically detected displacement assay |
| ET | electron transfer |
| FeAc | ferroceneacetic acid |
| HATU | *O*-azabenzotriazol-1-yl-tetramethyluronium hexafluorophosphate |
| HBTU | *O*-benzotriazol-1-yl-tetramethyluronium hexafluorophosphate |
| HPV | human papillomavirus |
| LCAA-CPG | long-chain alkylamine controlled pore glass |
| MEA | microelectrode array |
| MMTr | monomethoxytrityl |
| NHS | *N*-hydroxysuccinimide |
| pcb | printed circuit board |
| PCR | polymerase chain reaction |
| PEEK | polyetheretherketone |
| rCP | reference capture probe |
| rSP | reference signalling probe |

| | |
|---|---|
| SP | signalling probe |
| ss | single stranded |
| T | target |
| TEAA | triethyl ammonium acetate |
| THF | tetrahydrofuran |

## Introduction

Miniaturization technologies, which integrate engineering capabilities well established in the silicon microfabrication industry and microelectromechanical systems with expertise in molecular biology, allow molecular tests to be carried out on microchips [1].

Microarrays can be fabricated using a variety of technologies, including printing with fine-pointed pins onto glass slides, photolithography using premade masks [1], photolithography that replaces mask sets with a dynamic micromirror device [2, 3], ink-jet printing [4] as initially proposed by Blanchard and Hood [5], or electrochemistry on microelectrode.

Tremendous efforts have been made in the past decade to commercialize miniaturized instruments for molecular diagnostics, including thermocyclers, microfluidics chips, DNA microarrays, and other types of biosensors [6, 7].

Instead of detecting and studying one gene at a time, microarrays allow thousands or tens of thousands of specific DNA or RNA sequences to be detected simultaneously on a small glass or silica slide with an area of only 1–2 $cm^2$. Although the principles of specific DNA and RNA detection have remained unchanged, the greatly increased scale on which this can be achieved with DNA microarrays has made it possible to qualitatively tackle different questions in biology and medicine.

An integrated molecular testing system involves innovation at each step, such as sample collection, nucleic acid extraction/separation, gene amplification, and signal detection/analysis. The major emphasis in the development of miniaturization technologies has been on highly sensitive biosensors that can be integrated with new technologies in other steps. Electronic techniques are of particular interest for this purpose because they can be directly integrated with microelectronics and microfluidics systems to gain advantages in miniaturization, multiplexing, and automation.

Traditionally, molecular diagnostic detection has relied on fluorescent or radioactive labels, and signal transduction is performed with equipment that greatly increases size and cost of the whole system. Setups using fluorescence detection are widely commercially available, but there are a number of other detection techniques gradually emerging. Electrochemical methods are among the most popular electronic techniques that naturally interface the biomolecules in solutions with solid-state electronics [8]. Many reports have demonstrated individually addressed microelectrode arrays for molecular analysis [9–16]. However, the sensitivity of electrochemical detection based on microelectrodes is typically substantially lower than conventional laser-based fluorescence techniques [17–20], and several approaches have been employed to improve detection sensitivity such as redoxcycling [21, 22], carbon nanotubes, and semiconducting nanowires [23, 24].

At least for clinical or medical diagnostics, standard nucleic acid testing using an initial linear or exponential amplification of the targets, however, set a sensitivity benchmark that cannot and probably will not be met by any microarray detection technology. Therefore a state of the art nucleic acid detection on microarrays in this field will rest on preamplification of the targets. Therefore, sensitivity requirements for microarrays may be low and other needs like easy workflow and easy integration into standard procedures of routine clinical or medical diagnosis come to the fore.

Though sensitivity requirements for the detection of amplified nucleic acid targets are low, sensitivity and selectivity are still two of the most challenging criteria for the development of DNA biosensor devices.

In this paper an electrical detection technology will be introduced that is easy to handle, easy to integrate into automated diagnosis systems, but can also be applied in a conventional manner, e.g., as a sensor to detect PCR amplicons directly in the PCR reaction vessel.

## Materials and methods

### Microarray substrate and cleaning procedures

The microarrays used in this study are shaped as a "dipstick" that can be immersed into conventional tubes for direct detection of (PCR) amplicons (cf. Fig. 1). The actual microelectrode arrays (MEAs) at the bottom part of the stick consist of 32 square gold electrodes (70 μm× 70 μm) on Si with counter and (pseudo) reference electrodes (both gold) (photolithographically structured; vapor deposition of 99.99% gold on Si; and leads are sealed with $Si_3N_4$; manufactured by HL-Planartechnik, DE-Darmstadt). These arrays are bonded to printed circuit boards (pcbs) for electrical connection to a potentiostat. Bond pads and wires are isolated with glob-top (Emerson Cuming STYCAST epoxy glue, Polytec GmbH, DE), and the leads to the bond pads on Si are covered with $Si_3N_4$. At the pcb part of the stick a solder mask defines the bond pad diameter (100 μm) and covers the leads to the connector. Sliding contacts at both sides at the top of the dipstick can be hooked to a standard plug connector (type FH, Nr. 5177983-1 Tyco Electronics Ltd.).

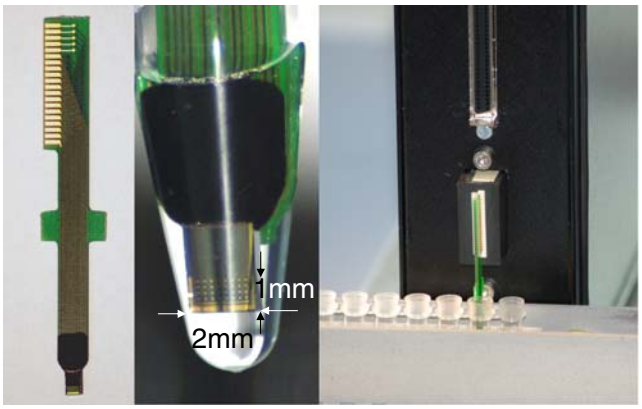


**Fig. 1** Photograph of the dipstick-type MEA (*left*) consisting of 32 gold-microelectrodes on Si (*bottom* part of the stick) that is connected to a standard sliding contact on pcb (macroscopic gold pads on the *upper left* part of the stick; an identical number of contacts is at the back of the stick) via wire bonding (mounted under the *black* epoxy glue, next to the Au-on-Si-MEA). The *middle photo* shows an enlargement of the Au-on-Si-MEA, when it is immersed in a standard 100-μL PCR tube. The *right-hand photo* shows the dipstick connected to the potentiostat

To precondition the MEAs for probe immobilization they were rinsed with water and ethanol and sonicated in ethanol for 5 min and subsequently cleaned with Ar plasma (Femto, Diener Electronic, DE, 2 min, power 3). Afterwards MEAs were subjected to an electropolishing procedure [25]: the electrodes were immersed in 1 M $H_2SO_4$, while performing at least three cyclic voltammetry (CV) cycles from 0 to 1.55 V vs. Ag/AgCl at 50 mV/s after being biased to 1.65 V for 10 s using a three-electrode configuration (the bare gold pseudoreference electrode on the MEA lies on a potential of about +0.15 V vs. Ag/AgCl in $H_2SO_4$, cf. Electrochemical analysis). Besides the cleaning effect of this treatment, it is possible to determine the real surface area of the electrodes by integration of the current of the reductive oxide stripping peak [26]. The electrodes in this study had a mean roughness of around 1.1. For the reduction of possible traces of gold oxide the MEAs were stored in ethanol for 15 min prior to further use.

For some electrochemical experiments commercial (Metrohm AG, CH-Herisau) gold disk electrodes with a diameter of 0.2 cm (encapsulated in PEEK) and/or of 0.3 cm (encapsulated in Teflon) were used (cf. Fig. 10). These electrodes were polished sequentially with a series of diamond slurries with gradually decreasing particle sizes (ranging from 15 μm, over 9 μm, 3 μm, 1 μm, 0.3 μm down to 0.1 μm) on a polishing pad. The electrodes were rinsed with ethanol and water after each particle size, followed by short sonication in ethanol. Before probe immobilization the electrodes were electropolished (see above).

## Synthesis of DNA oligonucleotides: capture and signalling probes, reference capture and signalling probes, and target mimics

For the incorporation of multiple labels or anchoring groups in the signalling or probe oligonucleotides, three different methods have been used:

(i) Up to four ferrocene labels have been incorporated at the 5′ end of the signal oligonucleotides by adding four aminolink phosphoramidites, deprotecting the amino groups on-column, and derivatizing the amino groups with ferrocene acetic acid.

(ii) One to four osmium labels have been added to the 5′ end of signal oligonucleotides utilizing a single 5′ amino group, amino acid-derived osmium compounds (compounds VIII and IX, Fig. 5), and standard peptide chemistry.

(iii) Three dithiolphosphoamidite (DTPA) anchoring groups have been added to the 3′ end of probe oligonucleotides by standard phosphoramidite chemistry using nonstandard synthesis blocks (compounds III and IV, Fig. 2)

### *Synthesis of probe oligonucleotides with three dithiolphosphoramidite (DTPA) groups at the 3′ end (compound I, Fig. 2)*

The synthesis strategy for DTPA and DTPA-modified oligonucleotides is illustrated in Fig. 2. Oligonucleotide synthesis has been carried out on an Applied Biosystems 394 DNA-synthesizer using standard procedures (users' manual) on a 0.2-μmol scale. Dimethylformamidine-protected deoxyguanosine amidite and 5-ethylthio-1*H*-tetrazole (ETT) activator were used. Target and probe oligonucleotides were prepared "trityl-on" and purified by reversed-phase high-performance liquid chromatography (RP-HPLC).

### *Modification of CPG (controlled pore glass)*

*Hemisuccinate of the monotritylated cyclodithioerythritol [27] (cyclo-DTE, compound II, Fig. 2)* Monotritylated cyclo-DTE (600 mg, 1.32 mmol; compound I, Fig. 2) is dissolved in dichloromethane. To this solution, cooled in an ice bath, 198 mg (1.98 mmol) succinic anhydride and 319.4 mg (1.98 mmol) 4-dimethylaminopyridine (DMAP) are added. The stirred reaction mixture is allowed to warm to room temperature and stirred overnight. After addition of 30 mL dichloromethane, the reaction mixture is extracted twice with 50 mL of 0.1 M phosphate buffer pH=5.0 and twice with 50 mL brine. The organic phase is dried over sodium sulfate and, after addition of 200 μL triethylamine, evaporated to a gum. The raw product is taken up in the minimum quantity of dichloromethane containing 1%

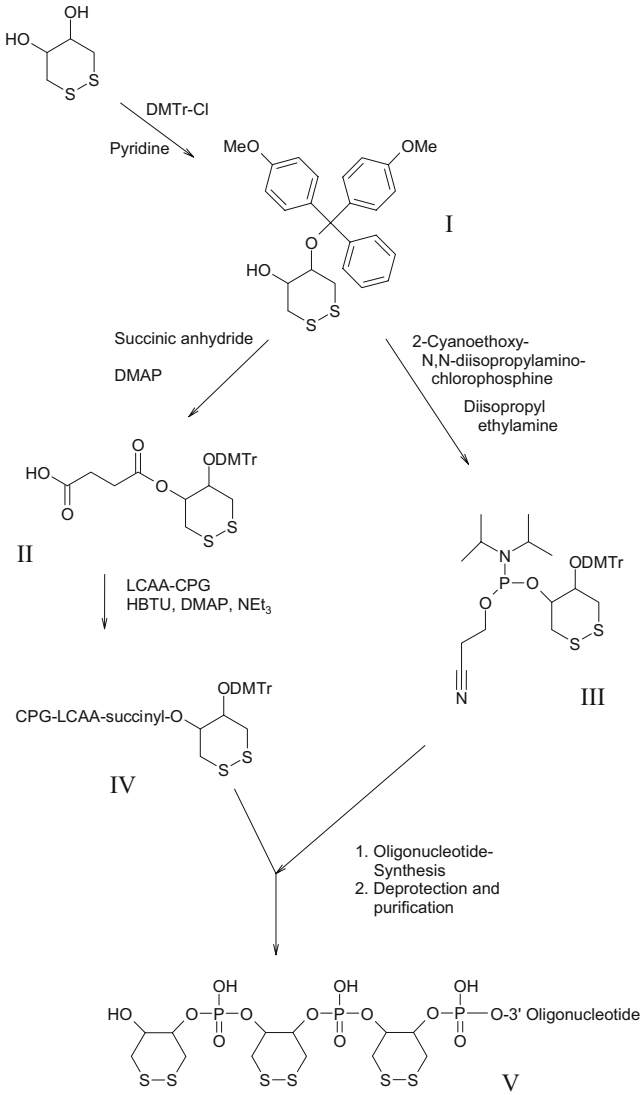


**Fig. 2** Synthesis strategy for dithiolphosphoamidite (DTPA, compound IV) and DTPA-modified oligonucleotides (for details see text)

triethylamine and chromatographed on silica gel 60 (0.063–0.2 mm) with dichloromethane, 1% triethylamine to dichloromethane, 2% methanol, 1% triethylamine. Yield 293 mg (0.529 mmol, 40%), mass spectrometry (MS) is as expected.

*Esterification of the LCAA-CPG [28] (long-chain alkylamine controlled pore glass) (compound IV, Fig. 2)* LCAA-CPG (1g), 49.2 mg (75 μmol) hemisuccinate (compound II), 27.5 mg (225 μmol) DMAP, 85.3 mg (225 μmol) HBTU (*O*-benzotriazol-1-yl-tetramethyluronium hexafluorophosphate), and 31.4 μL (225 μmol) triethylamine are shaken overnight in 5 mL dry acetonitrile. The CPG is filtered and washed four times with 20 mL acetonitrile, three times with 20 mL diethyl ether and allowed to dry in a fumehood. For determinating the loading of the CPG, about 5 mg is exactly weighed in a 25-mL volumetric flask and the dimethoxytrityl group is cleaved with 1 M toluene sulfonic acid in acetonitrile. By measuring the absorption at 498 nm, the loading may be calculated:

$$\text{Loading}\,(\mu\text{mol/g}) = (V_{\text{Detrit}} \times Abs_{498} \times 14.29)/m$$

| | |
|---|---|
| $V_{\text{Detrit}}$ | volume of detritylation solution in mL |
| $A_{498}$ | absorption at 498 nm |
| $m$ | weight of support in mg |

If the loading is sufficient (>40 μmol/g), unreacted aminogroups of the CPG are capped by shaking the CPG with a mixture of 3 mL cap A and 3 mL cap B for 30 min. The CPG is filtered and washed seven times with 20 mL acetonitrile.

*1,2-Dithiane-4-O-dimethoxytrityl-5-ol (compound I, Fig. 2)* The cyclo-DTE is dried for several days under high vacuum at room temperature. Under argon, 6 g (39.4 mmol) cyclo-DTE is dissolved in 45 mL dry pyridine. Dimethoxytrityl chloride (15 g, 44.27 mmol) is dissolved in 50 mL dry THF and added dropwise to the cyclo-DTE solution over 1–2 h at room temperature. The resulting solution is stirred overnight. The solution is evaporated to a syrup using a rotary evaporator; residual pyridine is removed by two coevaporations with 30 mL toluene. The residue is taken up in the minimum quantity of dichloromethane containing 1% of triethylamine and chromatographed on silica gel 60 (0.063–0.2 mm) with 10% ethyl acetate, 1% triethylamine in heptane to 20% ethyl acetate, 1% triethylamine in heptane. The resulting white powder is then chromatographed on 100 g of C18-RP silica gel (Chromabond C18 ec), using 10% 0.1 M TEAA pH 7.4 in acetonitrile. Product-containing fractions are pooled and concentrated under reduced pressure until the product precipitates. The product is then filtered and washed with water to eliminate residual TEAA. For the synthesis of the phosphoramidite, as well as for the synthesis of the hemisuccinate, the product should be dried thoroughly under high vacuum. Yield 10.7 g (23.6 mmol, 60%), MS as expected.

*1,2-Dithiane-4-O-dimethoxytrityl-5-[(2-cyanoethyl)-N,N-diisopropyl)]-phosphoramidite (DTPA [29], compound III, Fig. 2)* Under argon, 8 g (17.6 mmol) of the mono-tritylated cyclo-DTE (compound I, Fig. 2) is dissolved in 20 mL dry acetonitrile in a flask stoppered with a septum. The solution is cooled in an ice bath and 12.3 mL (70.4 mmol) of very dry diisopropylethylamine is added. Using a syringe, 4.8 mL (21.1 mmol) chloro-diisopropylamino-cyanoethoxy phosphine is added dropwise over 15 min. The mixture is stirred for 10 min at 0 °C, then the ice bath is removed and the reaction mixture is allowed to warm to room temperature. After stirring for 20 min, the reaction is stopped by addition of 1.5 mL dry methanol. The solution is evaporated to a syrup-like consistency, taken up in dichloromethane

with 1% triethylamine, and chromatographed on silica gel 60 (0.063–0.2 mm) with 7.5% ethyl acetate, 1% triethylamine in heptane to 15% ethyl acetate, 1% triethylamine in heptane. Yield 7.15 g (10.9 mmol, 62%), MS as expected.

Synthesis of probe oligonucleotides (compound V, Fig. 2) is done using the dithol-modifed CPG and coupling two additional dithiol groups to this support using 250 μL of 0.1 M DTPA in acetonitrile and 10-min coupling time for each addition (1-μmol scale). It is convienient, to carry out these two coupling steps on a large scale (1 or 10 μmol); the CPG modified with three dithio groups may be stored for several months under argon at −20 °C.

*Synthesis of ferrocene-modified signal oligonucleotides (compound VI, Fig. 3)*

To the 5′ end of the oligonucleotide, four consecutive Fmoc-protected C3 amino-linked phosphoramidites are added according to the manufacturer's recommendations except for omitting the capping steps, which results in a significantly higher yield for the ferrocene-modified oligonucleotide. The cleavage of the Fmoc, as well as the phosphate protecting groups, is accomplished by flushing the synthesis column for 5 min with 10% diethylamine in acetonitrile, then for 5 min with 0.1 M diazabicycloundecene (DBU) in acetonitrile solution. These solutions are installed instead of cap A and cap B after the synthesis on the machine. After this partial deprotection, the column is washed with acetonitrile for 2 min and dried in a stream of argon.

The dry support material is transferred into a screw-cap-type 1.5-mL reaction tube. For each 0.2-μmol synthesis, 11 mg (45 μmol) ferrocene acetic acid, 16.5 mg (135 μmol) DMAP, and 51 mg (135 μmol) HBTU are dissolved in a mixture of 150 μL acetonitrile, 50 μL DMSO, and 18.75 μL (135 μmol) triethylamine, added to the support and shaken for 2–3 h at room temperature in the dark. The support is then washed three times with 1.5 mL DMSO, three times with 1.5 mL acetonitrile, and dried in a speed-vac for 10 min. The modified oligonucleotides are cleaved from the support and deprotected by incubation with concentrated ammonia at room temperature overnight. The crude oligonucleotide is purified by RP-HPLC. Identity of the modified oligonucleotides was established by matrix-assisted laser desorption/ionization–time-of-flight (MALDI-TOF) mass spectrometry.

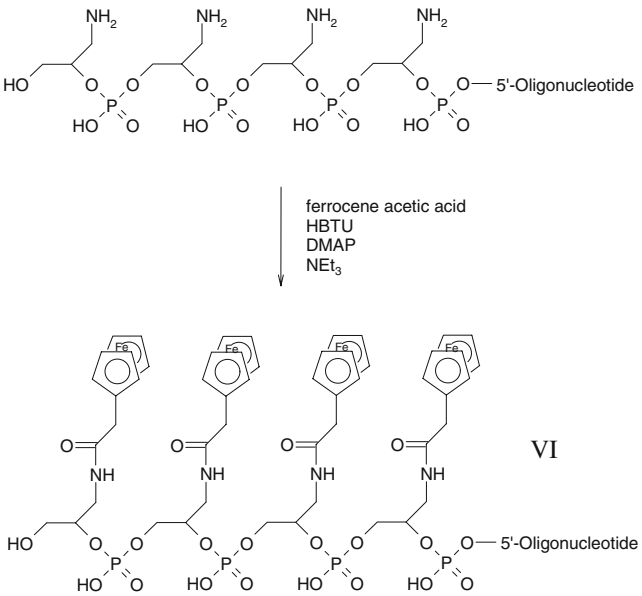


**Fig. 3** Synthesis of ferrocene-modified signal oligonucleotides (for details see text)

*Synthesis of osmium-modified signal oligonucleotides*

*Pyridylacryloyl-Fmoc-lysine (compound VII, Fig. 4)* Pyridylacrylic acid (1 g, 6.7 mmol) is suspended in 30 mL dry dioxane. *N*-Hydroxysuccinimide (772 mg, 6.7 mmol; NHS) and 1.45 g (7 mmol) dicyclohexylcarbodiimide are added. The mixture is stirred at room temperature for 4 h, then filtered from the precipitate, evaporated, and chromatographed on silica gel 60 (0.063–0.2 mm) with 80% ethyl acetate, 20% heptane). Yield 0.9 g (3.65 mmol, 54%).

Fmoc-D-lysine (1.05 g, 2.84 mmol) and 104 mg (0.85 mmol) DMAP are suspended in 30 mL dry pyridine and 0.7 g (2.84 mmol) of pyridylacrylic acid NHS-ester in 30 mL dry dioxane is added dropwise over 30 min. The mixture is stirred overnight. The solvent is evaporated under reduced pressure and the remainder coevaporated twice with 20 mL toluene. The solid is extracted with 40 mL 15% methanol in dichloromethane and filtered. The insoluble solid is unreacted Fmoc-lysine and may be reused. The filtrate is evaporated and chromatographed on silica gel 60 (0.063–0.2 mm) with 8% methanol in dichloromethane to 10% methanol in dichloromethane). Yield 0.63 g (1.26 mmol 44%), MS as expected

*Osmium complexes (compounds VIII and IX, Fig. 5)* Osmium-bis-*N*,*N*′-(2,2′-bipyridyl) chloride potassium hexachloroosmate(IV) was made according to Sargeson et al. [30]: 492 mg (0.86 mmol) osmium-bis-*N*,*N*′-(2,2′-bipyridyl) chloride and 0.9 mmol of the amino acid component (Fmoc-D-3-pyridylalanine or pyridylacryloyl-Fmoc-lysine) are heated at reflux under argon in 40 mL ethanol and 30 mL water for 7 h. The solvent is evaporated and the

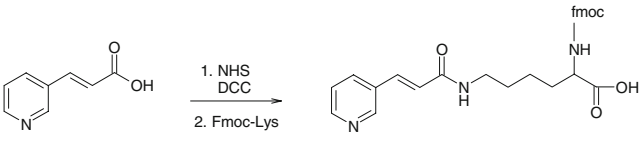


VII

**Fig. 4** Synthesis of pyridylacryloyl-Fmoc-lysine (for details see text)

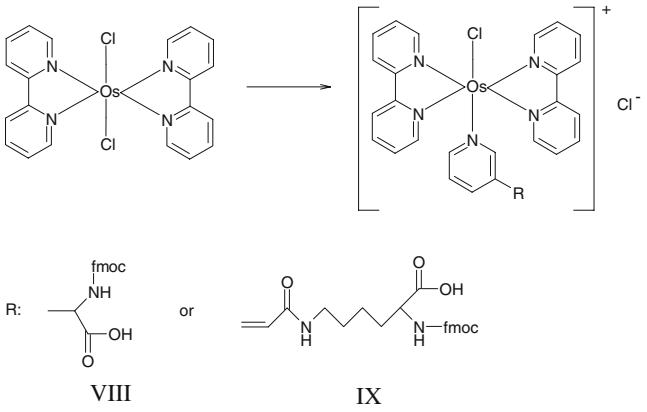


VIII IX

**Fig. 5** Synthesis of Os-modified oligonucleotides (for details see text)

residue chromatographed on silica gel 60 (0.063–0.2 mm) with 10% methanol in dichloromethane to 20% methanol in dichloromethane. Yield 50–70%, MS as expected.

*Coupling of the osmium complexes to oligonucleotides* The coupling was carried out on the fully protected oligonucleotides still bound to the solid support. The oligonucleotides were produced with a MMTr-protected $C_6$ aminolink, which was detritylated prior to coupling. The MMTr aminolink should be coupled without capping and the MMTr protecting group requires a prolonged detritylation time (3 min). The amino group should then be deprotonated by flushing the column with capB for 5 min, followed by washing with acetonitrile for 5 min and drying with argon. The support with the oligonucleotide is transferred into a 1.5-mL screw-cap-type reaction tube and suspended in 100 μL fresh and dry DMF. *O*-Aza-benzotriazol-1-yl-tetramethyluronium hexafluorophosphate (3.14 mg, 8 μmol; HATU) and 2.84 μL (16 μmol) diisopropylethylamine and 8 μmol of the osmium–amino acid complex were dissolved in 100 μL fresh DMF and preactivated for 1 min, then added to the support material suspension and shaken for 20 min. The support bound oligonucleotide is then washed with DMF and acetonitrile and either cleaved and deprotected with conc. ammonia for 15 h at room temperature or the Fmoc group of the osmium amino acid label is cleaved with 0.5 M DBU in acetonitrile for 15 min, and additional labels are added by repeating the coupling/Fmoc deprotection procedure. The crude oligonucleotides are purified by RP-HPLC. Identity of the modified oligonucleotides was established by MALDI-TOF mass spectrometry.

The sequences for a typical set of capture and signalling probes (CP, SP), reference capture and signalling probes (rCP, rSP), and target mimics (T) for HPV 6 is shown in Table 1: capture probes contain a spacing sequence 3′ to the detection sequence (separated by an underscore) that is not complementary to any targets of a certain assay. The capture probes are modified with three DTPA groups at the 3′ end. Signalling probes are modified with one to four ferrocenium groups at the 5′ end.

### *Immobilization of DNA capture and signalling probes onto the MEA*

The capture probe monolayers on gold were prepared immediately after electropolishing by contact printing (equipped with split pins, 90-μm footprint) with closed gadget at 80% relative humidity. Capture probes (50 μM) were dissolved in 125 mM $Na_2SO_4$ and were spotted onto the electrodes in the desired pattern. After spotting, the arrays stayed in the gadget for 1 h, were rinsed with water, and postprocessed with ω-HO-undecanethiol (1 mM in EtOH) for 3 h, rinsed with ethanol and water, incubated with ω-HO-hexanethiol (1 mM in 10 mM phosphate buffer, pH=7), finally rinsed with 10 mM phosphate buffer, pH=7, and dried in an Ar stream. Wrapped MEAs with capture probes immobilized according to this procedure were stable for at least 1 year (data not shown). The complexation of capture probes on these MEAs with complementary signalling probes was accomplished either by a spotting procedure as described (without postprocessing) or by incubating the MEAs with a mixture of all necessary signalling probes (50 nM each, in 250 mM $Na_2SO_4$) for 0.5 h and subsequent rinsing (10 mM phosphate buffer, pH=7) and drying (Ar stream). MEAs

**Table 1** 5′ to 3′ sequences for capture and signalling probes (CP, SP, complementary sequences are in *italics*), reference capture and signalling probes (rCP, rSP, complementary sequences are in *italics*), and target mimics (T, complementary to the signalling probe SP) for HPV 6

| Probe or target mimic | Sequence |
|---|---|
| CP_HPV-6 | *TCCGTAACTACATCTTCCACATACACCAA*_CATATTTATT |
| SP_HPV-6 | *TTGGTGTATGTGGAAGATGTAGTTACG*_GATGTACATAATGTCATGT TGGTACTGCG |
| rCP_HPV-6 | *AACCACATTCACCTTCTACATCTATGCCT*_CATATTTATT |
| rSP_HPV-6 | *AGGCATTGATGTAGAAGGTGTATGTGGTT*T |
| T_HPV-6 | TGGTAGATACCACACGCAGTACCAACATGACATTATGTACATCCGT AACTACATCTTCACATACA CCAATTCTGA |

with capture and signalling probes immobilized are currently being tested for stability but they are stable for at least a month (data not shown).

## Amplification reactions

DNA of clinical specimens were isolated by standard procedures according to the manufacture's protocols using a DNeasy Blood & Tissue kit (Qiagen N.V.). The PCR protocol includes two subsequent PCR amplifications with Fw-6 and Rev-6 for amplification of HPV type 6 (Fw-6 ATAATGGCHCAGGGACATAACAATGG/Rev-6 ATTAAGCGTCCMARRGGATACTGATC). In the first amplification reaction a PCR product was produced, using 10 μL of the DNA preparation, to amplify the sample with 30 pmol (each) of Fw-6 and Rev-6 in 100 μL 16 mM ammonium sulfate, 100 mM Tris/HCl pH=8.3, 3 mM $Mg^{2+}$, 200 μM (each) dATP, dCTP, dTTP, and dGTP as buffer, and 1u Immolase DNA polymerase (Bioline). After 10 min denaturation and heat activation of the enzyme at 96 °C, six cycles of a touch down protocol with decreasing annealing temperature starting at 57 °C and ending at 47 °C, each cycle with 1 min @ 96 °C, 30 s annealing, and 1 min @ 72 °C, followed by 30 amplification cycles with 30 s @ 96 °C, 30 s @ 56 °C, and 30 s @ 72 °C, and followed by a last synthesis step with 10 min @ 72 °C. The amplification mixture was stored at −20 °C. This amplification product was used (diluted by 1/10,000, 5 μL) as template for the preparation of single stranded products with an asymmetric PCR protocol. In this protocol 2 pmol of the Rev-6 and 40 pmol of Fw-6 were used in 100 μL 16 mM ammonium sulfate, 65 mM Tris/HCl pH=8.8 , 3 mM $Mg^{2+}$, 200 μM each of dATP, dCTP, dTTP, and dGTP as buffer with BioTaq DNA polymerase (Bioline). After 2 min denaturation at 96 °C, 35 amplification cycles with 30 s @ 96 °C, 30 s @ 56 °C, and 30 s @ 72 °C were performed. For the experiments ten tubes of each PCR product were pooled, precipitated, and quantified photometrically according to literature procedures [31], to get homogenous material for a series of experiments.

## Chemicals

Chemicals for DNA synthesis were from ABI, Germany (phosphoramidites, preloaded supports), Proligo Biochemie, Germany (LCAA-CPG), Glen Research, USA (MMTr $C_6$ Aminolink amidite), Chem Genes, USA (Fmoc $C_3$ aminolink), Mallinckrodt Baker, Germany (acetonitrile, activator ETT, oxidizer 0.02 M, detritylation solution, cap A, cap B), Biosolve, The Netherlands (dichloromethane), Machery-Nagel, Germany (C18 RP Silica), IRIS Biotech, Germany (HBTU, cyclo-DTT, DMAP, Fmoc-D-3-pyridylalanine), Sigma-Aldrich, Germany (*trans*-3-(3-pyridyl)acrylic acid, diisopropylethylamine), Merck Biosciences, Germany (HATU), and Acros, Belgium ($K_2OsCl_6$). All other chemicals were from VWR/Merck, Germany. All other chemicals used in this study, alkanethiols (propanethiol and hexanethiol), ω-hydroxyalkanethiols (hydroxyundecanethiol, hydroxpropanethiol, and hydroxyhexanethiol), NaCl, $Na_2SO_4$, NaOH, $H_2SO_4$, TRIS, and ethanol, were purchased from Fluka and were utilized as received. All buffer solutions were prepared using doubly distilled ultrapure water (Bamstead Nanopure Life Science).

## Hybridization

Hybridization (amplicon detection) can be performed directly after amplification by immersing the dipstick into the tube containing the amplicons, e.g., the PCR tube. Hybridization is followed on-line by electrochemical detection. To decrease detection time, elevated temperature or a temperature gradient is used during hybridization. In general each potential hybridization is monitored vs. a reference, i.e., relative to an electrode derivatized with capture/signalling probe hybrid that has an identical but inverse base sequence (see above) and thus cannot interact with the expected amplicon(s). Dehybridization was performed by incubating the MEA in 0.1 M NaOH for 10 min, subsequently rinsing the MEA with doubly distilled water, and finally drying the MEA (Ar stream).

## Electrochemical analysis

The electrochemical (EC) measurements were performed with a three-electrode setup in an appropriate electrolyte (indicated in the respective experiments). For single electrodes the typical setup was gold disk working electrode, Pt counter electrode, Ag/AgCl/3 M KCl reference electrode hooked to a AUTOLAB12 potentiostat (electrodes and potentiostat were purchased from Metrohm AG, CH-Herisau) equipped with an FRA2 impedance module, a SCAN-GEN module for the generation of true linear ramps, an ADC750 module for time resolution down to 1.3 μs, and an ECD module for low current measurements. Alternating current voltammetry (ACV) and (staircase) cyclic voltammetry (CV) experiments were designed as suggested by the manufacturer and in accordance with standard literature [32].

EC measurements of MEAs were performed either on the AUTOLAB12 with on-chip gold counter electrode and external Ag/AgCl/3 M KCl or on-chip gold reference electrode. If the gold on-chip reference electrode was used, 50 nM $Os(bipy)_2Cl_2$ was used as internal reference system. To electronically address the 32 individual gold microelectrodes a homemade multiplexer (MUX-96) [33] was used to serially switch between the individual working electrodes. Alternatively a homemade 32-fold potentiostat

(MP-32) [34] was used to address the 32 working electrodes in parallel. With MP-32 the standard setup consisted of the on-chip gold counter electrode, the on-chip reference electrode, and 50 nM $Os(bipy)_2Cl_2$ as internal reference system (the reversible oxidation/reduction of $Os(bipy)_2Cl_2$ occurs at $E_0 \approx 0$ V vs. Ag/AgCl). During hybridization/detection the temperature of the reaction vessel (PCR tube) with immersed MEA dipstick is controlled by a homemade heating unity [35] that is part of the MP-32.

EDDA detection principle

The EDDA detection principle [26, 36] established to directly detect hybridization in, e.g., a PCR tube, is illustrated in Fig. 6. After processing the MEA according to the probe immobilization guidelines described above the individual working electrodes (or test sites) consist of a hybrid between capture and signalling probes. The signalling probe is complementary to the expected target amplicons generated

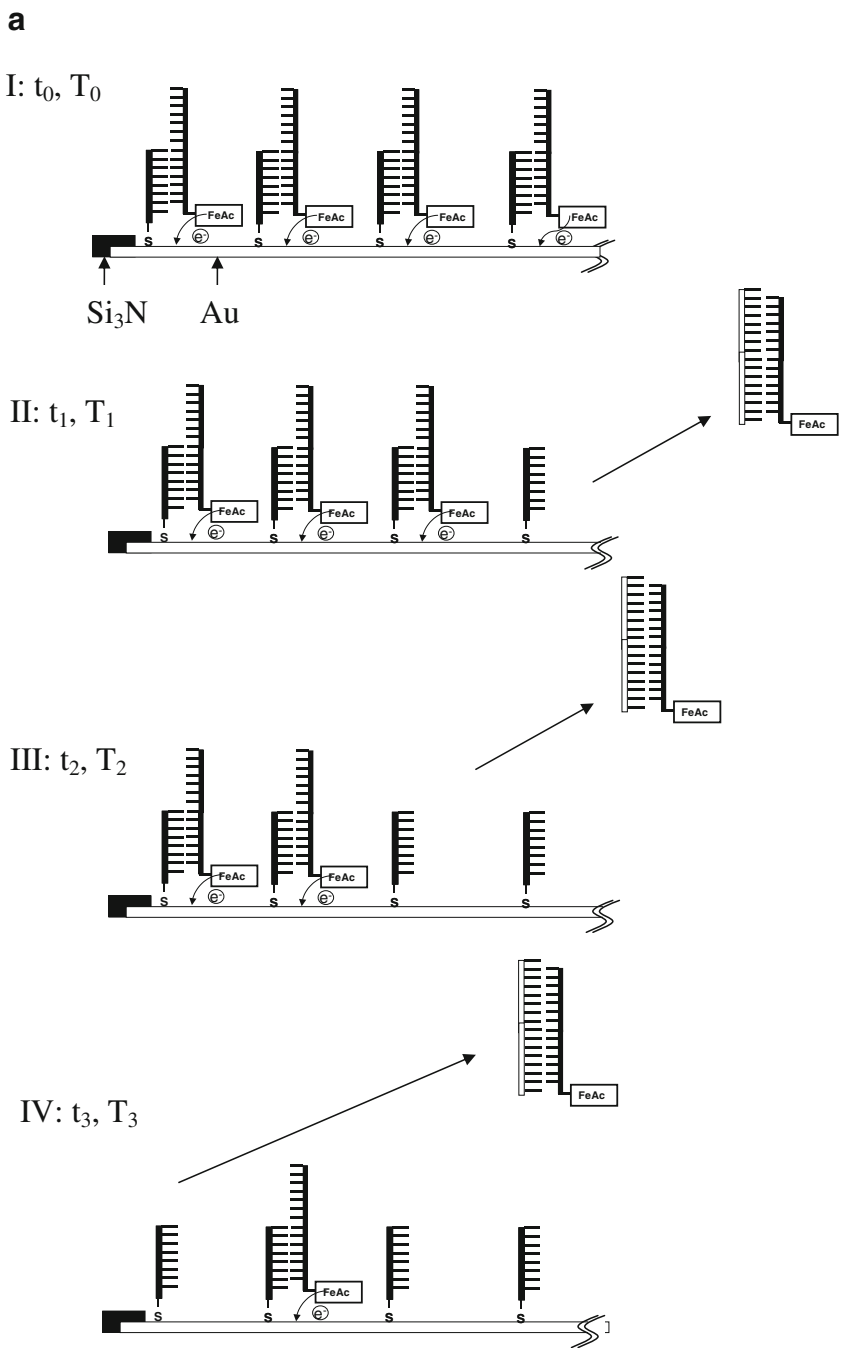


**Fig. 6** **a** Schematic representation of the EDDA process (for details see text). **b** Hypothetical curve progression of the electrochemically detected FcAc oxidation signal according to a processes illustrated in **a** (for details see text)

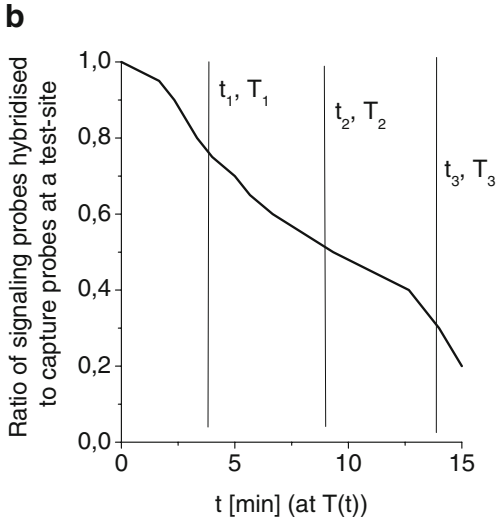


**Fig. 6** (continued)

during the asymmetric PCR. The electrode distant end of the signalling probe is not involved in hybridization to the capture probe but serves as a docking station to targets. At the electrode proximal ends the signalling probes carry covalently attached ferrocenium moieties depicted as FcAc in a closed frame (up to four moieties). These moieties can be oxidized at about 0.25 V vs. Ag/AgCl in any suitable electrochemical detection process (indicated by the encircled $e^-$ at the bent arrow between FcAc and the electrode surface). The corresponding signal is indicative for the full functionality of the test site on the one hand and a completely not hybridized state on the other hand (cf. Fig. 6 top line at $t_0/T_0$ and Fig. 7 at $t_0/T_0$).

Target amplicons may dock at the remote end of the signalling probe that is designed to be a perfect match to the target and eventually will completely hybridize with the signalling probe, thus releasing the signalling probe from the immobilized capture probe. The newly built hybrid of signalling probe and target amplicon will diffuse in solution. The concentration of these solution dissolved hybrids may stay quite low during the complete process, since the amount of surface-bound signalling probes is low (about $4\times10^{-16}$ mole per test site, see below) thus favoring the process of target-induced removal of signalling probes (cf. figure lines for $t_1/T_1$ to $t_3/T_3$).

The hybridization/detection process can be improved at elevated temperature. A hypothetical curve progression of the electrochemically detected FcAc oxidation signal according to the processes illustrated in Fig. 6 is depicted in Fig. 7.

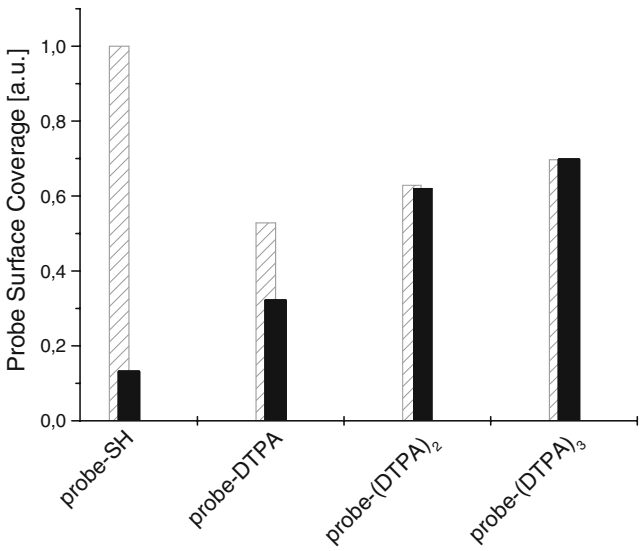


**Fig. 7** Capture probe oligonucleotide surface coverage as a function of the number of thiol anchoring groups (i.e., one for probe-SH, two for probe-DTPA, four for probe-$(DTPA)_2$, and six for Probe-$(DTPA)_3$) after spotting (*dashed bars*) of the probe and after postprocessing with ω-HO-hexanthiol (*black bars*)

## Results and discussion

### Test site characterization (stability, activity, surface coverage)

The immobilization of nucleic acids onto substrates is complex and crucial to the performance of the microarray, since (i) the capture probe has to form a stable bond to the substrate, (ii) the spacing of the capture probes has to allow specific binding of the target, (iii) nonspecific adsorption of the material to be arrayed has to be prevented.

Chemisorption of thiols on gold (electrodes) is a common and simple procedure to immobilize probes on a surface. The gold–sulfur bond with a binding energy of about 30–45 kcal/mol [37] (cf. at least 100–150 kcal/mol for a covalent bond [29]) is relatively weak in order to anchor a biopolymer onto a surface. As reported, monofunctional thiol-terminated oligonucleotides immobilized on a surface slowly decompose at temperatures between 60 and 90 °C and in the presence of buffers with high salt concentration [38] and are almost completely displaced from the surface when treated with biological buffer systems containing, e.g., dithiothreitol or mercaptoethanol [39, 40].

We used different thiol anchoring groups for the immobilization of capture probe oligonucleotides, followed by passivation of remaining gold sites with short-chain thiols. Besides electrochemical passivation of the electrode surface, postprocessing with short-chain thiols reduces background capacitive currents and nonspecific adsorption. To enable direct electrochemical access to the immobilization process, the 20-base-long capture probes were covalently modified with Os complex at the remote end (cf.

Materials and methods). The coverage with capture probes is then easily determinable by CV via the integrated oxidation peak.

As depicted in Fig. 8, the number of thiol anchoring groups per capture probe is essential to surface coverage and stability of immobilized probes. Though the coverage is highest for singly HS-anchored probes, these probes are largely displaced from the surface by short-chain thiol postprocessing, most probably due to removal of unspecific and/or displacement of weekly bound probes. Using multiple anchoring of the probes via DTPA units with two HS groups per unit reduces the spontaneous surface coverage to some extent, but the immobilized probes are increasingly more stable towards postprocessing with increasing number of anchoring groups as indicated by the decreasing displacement of capture probes due to thiol postprocessing with increasing numbers of HS anchoring groups per capture probe. Best results are obtained in this series for capture probes with three DTPA groups (corresponding to six HS anchoring groups).

To simulate stability towards mechanical stress and potential reusability Au-electrode-based sensors were treated with NaOH (a typical dehybridization procedure), hybridized, dehybridized, and rehybridized. The surface coverage change (determined as above) for different thiol anchoring groups due to this "stress procedure" is compared in Fig. 9. Again stability/reusability increases with increasing number of thiol anchors per capture probe. The results depicted in Figs. 8 and 9 were reproducible in a series of experiments (experiments were repeated at least ten times with different electrodes. Mean deviation is shown in Fig. 9 and was less than 10% for the experiments shown in Fig. 8). Additionally, postprocessing was tested with different alkanethiols (C-2 to C-11, each $CH_3$-terminated or $CH_2OH$-terminated) resulting in an optimized procedure for optimal capture probe immobilization by using threefold DTPA-modified capture probes and subsequent posttreatment with ω-HO-undecanthiol in EtOH and a final treatment with ω-HO-hexanthiol in aqueous buffer [41].

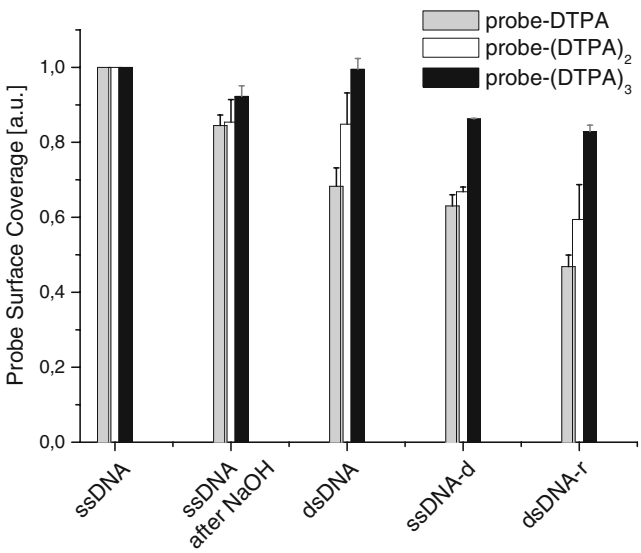


**Fig. 8** Capture probe oligonucleotide surface coverage after probe immobilization and posttreatment (ssDNA), after additional incubation in 0.2 M NaOH for 10 min (ssDNA after NaOH), after subsequent first hybridization (dsDNA), dehybridization (ssDNA-d), and rehybridization (ds-DNA-r) for differently anchored capture probes (as indicated in the figure)

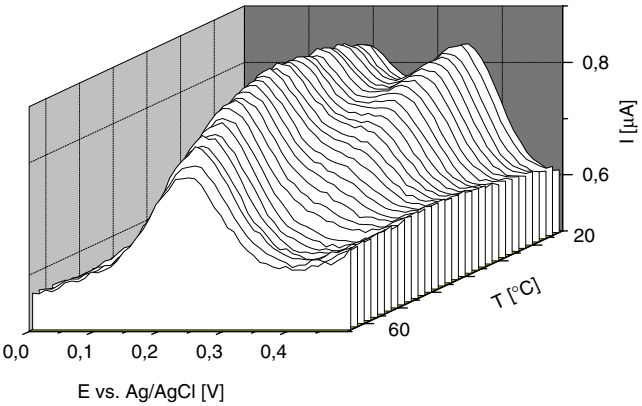


**Fig. 9** ACV (10 Hz, $E_{ac}$=20 mV) of surface-immobilized Os-modified capture probe (peaking at +200 mV) hybridized with doubly ferrocenium-modified signalling oligonucleotide (peaking at +350 mV) against temperature (20–65 °C)

The experiments with Os-modified capture probes enable absolute quantification of surface coverage. The coverage has to be as high as possible to ensure a maximum of detectable hybridization events but is restricted to a capture probe density where probes are still accessible by target oligonucleotides. Literature values for oligonucleotide surface densities range from $1–4\times10^{12}$ molecules/cm$^2$ for oligonucleotides shorter than 24 bases [42–44] to $6–9\times10^{12}$ molecules/cm$^2$ [45, 46]. In a series of experiments the optimum was adjusted by variation of buffer composition, capture probe concentration, and immobilization incubation time using the above findings for an optimized capture probe anchoring. As a result an optimized value around $4\times10^{12}$ molecules/cm$^2$ ($\pm1.5\times10^{12}$ molecules/cm$^2$) was obtained (vide infra).

In a two-label experiment under these optimized immobilization conditions the capture probe was modified with one 5′-osmium complex at the remote end and the complementary signalling oligonucleotide was labelled with two 5′-ferrocene carboxylic acid moieties (in vicinity of the electrode). In Fig. 9 the melting behavior of a hybrid between capture and signalling oligonucleotide is followed by alternating current voltammetry (ACV). The osmium complex having a peak at +200 mV (vs. Ag/AgCl/3 M KCl) is well separated in

potential by 150 mV from the ferrocene carboxylic acid peak at around +350 mV.

A rough calculation of the surface concentrations of capture probe and target according to O'Conner et al. [Eq. (1)] [47] results in $3\times10^{12}$ molecules/cm$^2$ and an accessibility of capture probes for signalling oligonucleotides of around 50%.

$$I_{\mathrm{avg}}(E_0) = 2zlfF\Gamma A \cdot \frac{\sinh\left(\frac{zFE_{\mathrm{ac}}}{RT}\right)}{\cosh\left(\frac{zFE_{\mathrm{ac}}}{RT}\right)+1} \quad (1)$$

| | |
|---|---|
| $\Gamma=nA$ | surface concentration |
| $E_0$ | Nernst potential, formal potential |
| $E_{\mathrm{ac}}$ | amplitude of ac voltage |
| $R$ | universal gas constant |
| $T$ | absolute temperature |
| $n$ | amount of substance |
| $z$ | number of electrons for redox reaction |
| $l$ | number of labels per molecule |

The above analysis of surface coverage and capture probe accessibility does not take into account that peak heights in ACV depend on the actual heterogeneous electron transfer rate ($k_{\mathrm{ET}}$) of the recorded electrochemical label. Peak heights of the ACV increase with increasing frequency until the frequency matches $k_{\mathrm{ET}}$. As depicted in Fig. 10 the frequency dependence of the ACV peak heights of Os-labelled capture probe and ferrocenium-labelled signalling probe differ significantly, indicating a significantly higher $k_{\mathrm{ET}}$ for the electrode proximal ferrocenium labels compared with the electrode distant Os label. A more rigorous approach is based on electrical impedance spectroscopy data of the two-label experiments [48]. There the surface coverage and accessibility of the capture probes immobilized under optimized parameters resulted in a coverage of about $4\times10^{12}$ molecules/cm$^2$ ($\pm$ $1.5\times10^{12}$ molecules/cm$^2$) and an accessibility of >85%.

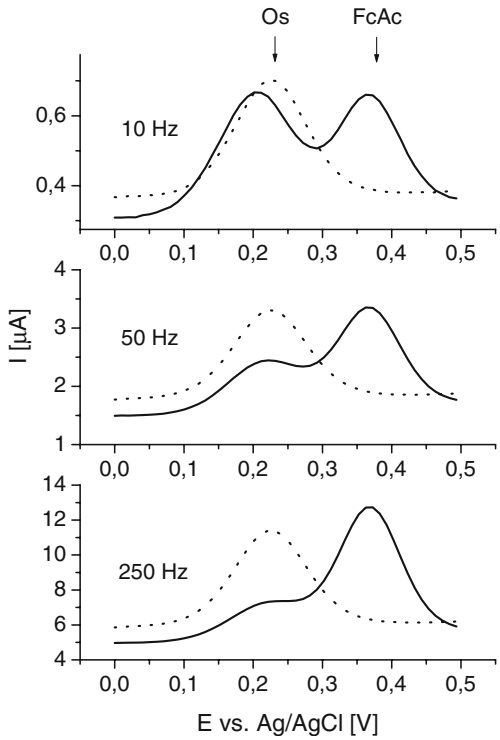


**Fig. 10** ACV ($E_{\mathrm{ac}}$=20 mV) of surface-immobilized Os-modified capture probe (peaking at +220 mV) hybridized with doubly ferrocenium-modified signalling oligonucleotide (peaking at +370 mV) at different ACV frequencies: *top* 10 Hz, *middle* 50 Hz, *bottom* 250 Hz. The hybridized (dsDNA) state is shown as *solid line*, the dehybridized state (ssDNA) as *dashed line*

## EDDA application: genotyping assay to analyze human papillomavirus (HPV) infections

Epidemiological and molecular studies over the past two decades have demonstrated convincingly that certain types of HPVs are etiologically related to the development of most cases of cervical cancer [49], the second most common cancer affecting women. There are at least 100 types of HPV that can be discriminated by genotyping. Women infected with high-risk HPV, such as HPV types 16, 18, 31, 33, and 35 are considered to be at a higher risk for the development of cervical cancer than those not infected with HPV or infected with low-risk HPV types, such as HPVs 6 and 11 [50].

We are currently establishing a HPV assay based on multiplexed PCR and subsequent analysis of the PCR product on a 32 test site microelectrode array (MEA) in EDDA format covering probes for all relevant high-risk HPV types and some low-risk HPV types. The dipstick (cf. Microarray substrate and cleaning procedures) carrying the MEA with capture/signalling probe hybrids is applied directly to the PCR solution and detection of screened genotypes started immediately (cf. EDDA detection principle).

In Fig. 11 typical electrochemical responses (here cyclic voltammograms, CVs) of the individual MEA test sites are shown for illustration purposes. The 32 microelectrodes contain capture probe/signalling probe hybrids for 15 different HPV genotypes and their corresponding reference (Ref) test site (see Materials and methods), two of them were coincidently not connected (electrodes two and four), one (number 21) is a control test site (no probes immobilized), two were spotted as duplicate (numbers 25 and 26). Initial current peak heights (black curves) that correspond to the absolute amount of capture probe/signalling probe hybrids at the individual test sites differ by a factor of about 2. This is probably due to a different capture probe immobilization behavior for different probe sequences and/or different accessibility of the different capture probe sequences to the signalling probes [51]. Hybridization between targets and

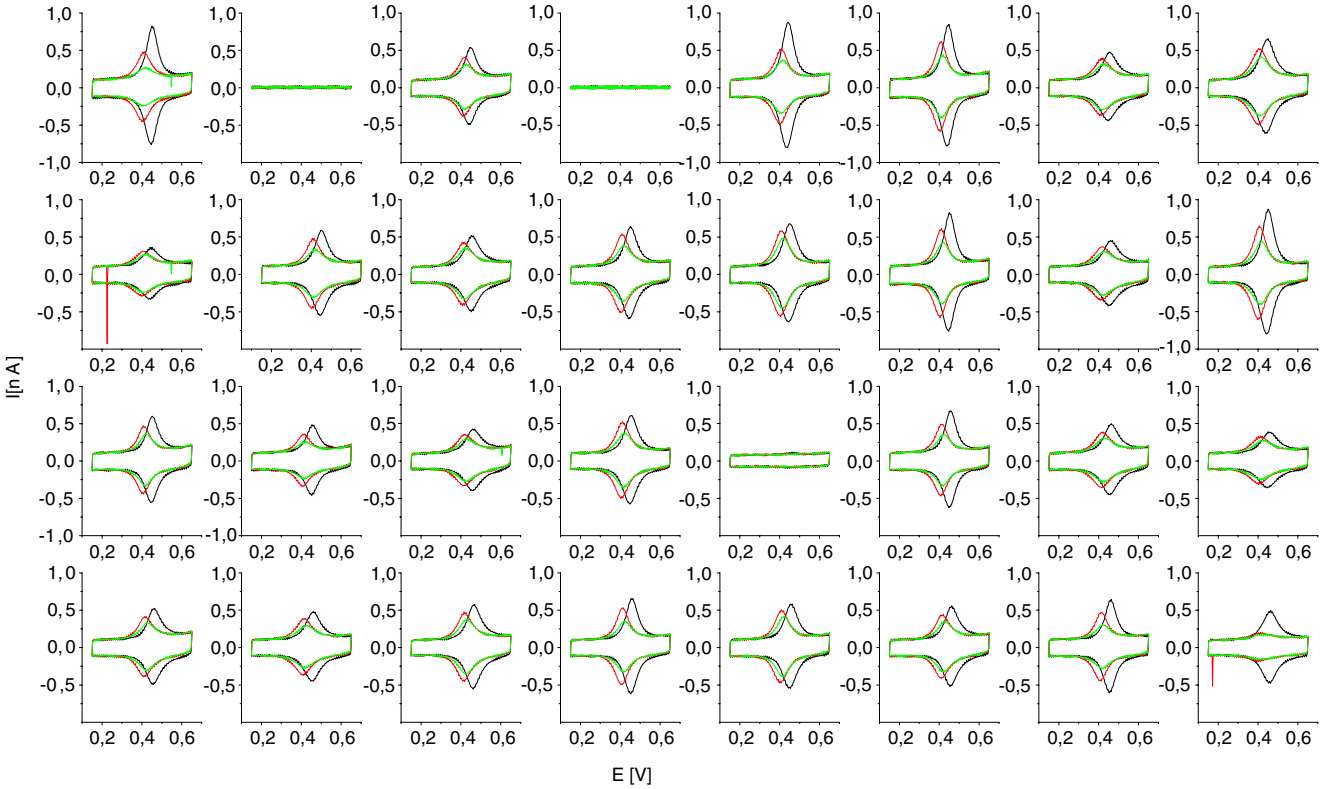


**Fig. 11** CV (scan rate 500 mV/s, *E* vs. internal $Os(bipy)_2Cl_2$ reference) of an ensemble of different surface-immobilized HPV capture probes hybridized with fourfold ferrocenium-modified signalling oligonucleotides during hybridization with a mixture of HPV target mimics ($c$=1 nM). *Black lines* are recorded at the beginning of hybridization ($t$=0, $T$=26 °C, *red* and *green lines* during hybridization ($t$=6 min, $T$=38 °C, *red lines*; $t$=10 min, $T$=46 °C , *green lines*). Electrodes 2 and 4 were not connected and electrode 21 carries no probes (control test sites to check for nonspecific effects, especially nonspecific immobilization of probes). Numbering of electrodes is line-by-line starting from the *top left*. Variations in peak potentials are due to the use of a pseudoreference electrode on the one hand and the differing temperatures on the other hand

signalling probes is supported by applying a temperature gradient to the PCR solution. Therefore, initial current signals are decreased gradually due to (i) the melting behavior of capture/signalling probes on the actual HPV test site or its reference test site and—in the case of the actual HPV test sites—this decrease is superimposed by the functional decrease due to hybridization between signalling probes and targets causing an additional displacement of the signalling probes from the test sites.

The electrochemical responses that are shown in Fig. 11 are for the whole array, but reponses at only three temperatures were analyzed in more detail over the complete temperature range observed: hybridization is followed on the microelectrode(s) while a temperature gradient of 2 °C/min is applied to the PCR solution and the CVs of the capture probe/signalling probe hybrids are recorded. A typical evaluation of the superposition of melting behavior and signalling probe displacement is shown in Fig. 12 for one test site and its reference (HPV 6 and Ref, respectively).

In Fig. 12 the integral of the currents obtained during CV are shown vs. temperature. Values are normalized to the initial value at $t$=0, individually for the actual HPV test site and the reference test site. The applied temperature gradient results in a gradual melting of the capture probe/signalling probe hybrids as can be observed by the decrease of the normalized signal for the reference test site that cannot interact with the target (cf. corresponding curves in Figs. 12a and b). In the absence of target the actual HPV-6 test site shows identical behavior to the reference test site indicating that the reference is well chosen. Repeating that hybridization with a hybridization solution containing HPV-6 target results in signal as displayed in Fig. 12b. The reference test site shows unchanged behavior, as compared to the situation without target displayed in Fig. 12a, whereas the signal for the actual HPV-6 test site decreases significantly faster with temperature due to target-induced displacement of the signalling probe. Hybridization with a modified HPV-6 target exhibiting at least two mismatches results in less than 10% target-induced displacement of the signalling probe as compared to the perfect-matching HPV-6 target.

Once curve progression of the "1-Hybridization" signal of probe and reference test site are known, hybridization can be

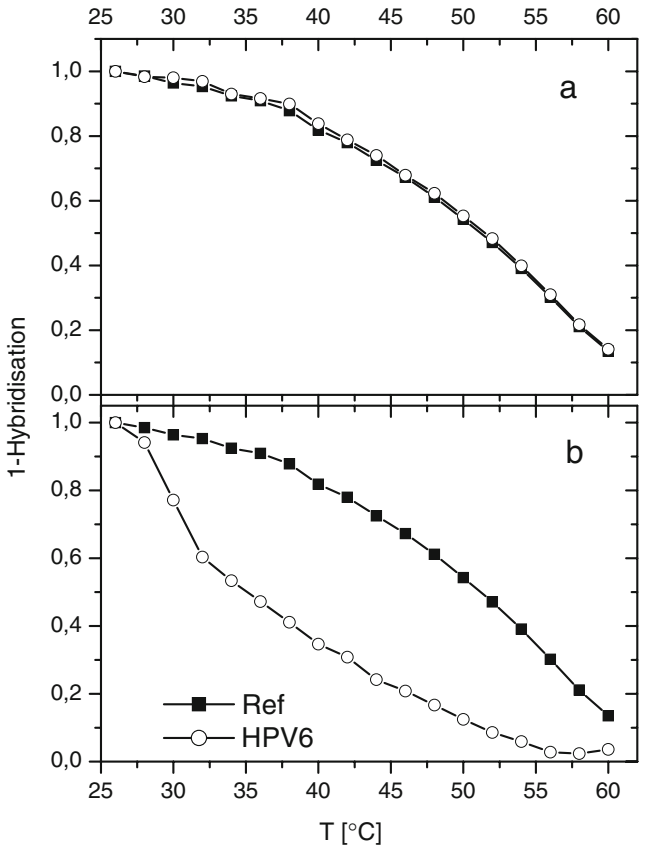


**Fig. 12** Displacement analysis for HPV type 6. Comparison of melting and displacement behavior of the actual test site (HPV-6) to a reference test site on the microarray (Ref) that shows identical melting behavior but whose can signalling probe cannot be displaced by targets. 1-Hybridization is the integral of the currents obtained during CV (scan rate 500 mV/s, *E* vs. internal $Os(bipy)_2Cl_2$ reference) as a function of time (and temperature). During hybridization a temperature gradient of 2 °C/min is applied to the PCR solution. Values are normalized to the initial value at $t=0$. **a** Analysis with PCR solution containing no HPV type 6 amplicon. **b** Analysis with PCR solution containing HPV type 6 amplicon (obtained from clinical material in a standard PCR reaction), diluted by a factor of 3

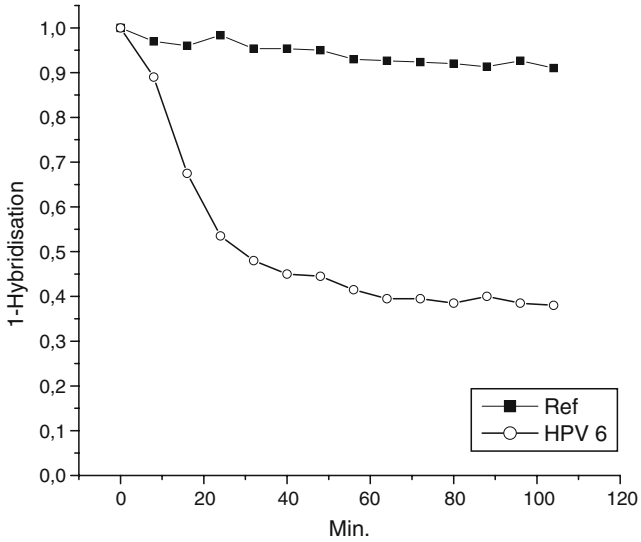


**Fig. 13** Displacement analysis for HPV type 6. Comparison of actual test site (HPV6) to a reference test site on the microarray (Ref) at the hybridization temperature with maximum deflection (here ca. 45 °C) between probe and reference site signal (see text). All other parameters are the same as for Fig. 12

performed at the temperature of maximum deflection (between probe and reference site signal approximately 45 °C in Fig. 12). In Fig. 13 this is shown for the HPV-6 test site and its reference. It is an alternative recording and visualization mode of the hybridization analysis enabled by EDDA ( "1-Hybridization" vs. time at 45 °C instead of "1-Hybridization" vs. temperature). Thus, in the final test format it is not necessary to spot and record the reference test site because reference behavior is known and all 32 test sites can be used for genotyping.

As already mentioned sensitivity requirements for nucleic acid analysis on microarrays are low for applications in medical diagnosis, since it is mandatory to perform an amplification reaction before microarray detection. Nevertheless we checked sensitivity with artificial targets (120-base-pair targets matching perfectly) and with PCR products. With artificial targets a recordable deviation between reference test site and HPV test site of more than 10% (the selectivity threshold) is obtainable for a 30 pM target solution. Typical PCR product [52] can be diluted by a factor of 10 to get such a recordable deviation between reference test site and HPV test site of more than 10%.

It should be noted that both selectivity and sensitivity are not only an issue of detection format but also are influenced by hybridization length, temperature, salt concentration, secondary structures of the target, state of the target (double strand or single strand) etc. and can/must be adopted to the actual assay (including amplification procedure and parameters) for medical diagnosis purposes.

## Summary

We have introduced a new electronic microarray format (EDDA) that can display hybridization of amplicons within a few minutes. The microarray can be applied directly to the amplification reaction. The minimal equipment needed mean that it is suited for clinical and medical diagnosis tests and is easy to handle. Moreover, there is no need for labeling or washing steps. The basic features of the microarray were characterized and a typical example for a medical diagnostic test was given. EDDA shows a sensitivity and selectivity very appropriate for the analysis of PCR products.

**Acknowledgements** Part of this work was financially supported by a governmental grant (sponsored by bmbf, program BioChance plus, grant 0313611A) which is gratefully acknowledged.

## References


1. Affymetrix (2007) http://www.affymetrix.com. Accessed 5 Dec 2007
2. Gao X, LeProust E, Zhang H, Srivannavit O, Gulari E, Yu P, Nishiguchi C, Xiang Q, Zhou X (2001) Nucleic Acids Res 29:4744–4750
3. Singh-Gasson S, Green RD, Yue Y, Nelson C, Blattner F, Sussman MR, Cerrina F (1999) Nat Biotechnol 17:974–978
4. Lausted C, Dahl T, Warren C, King K, Smith K, Johnson M, Saleem R, Aitchison J, Hood L, Lasky SR (2204) Genome Biol 5: R581–R58
5. Blanchard AP, Kaiser RJ, Hood LE (1996) Biosensors Bioelectron 11:687–690
6. McGlennen RC (2001) Clin Chem 47:393–402
7. Ramsay G (1998) Nat Biotechnol 16:40–44
8. Kerman K, Kobayashi M, Tamiya E (2004) Meas Sci Technol 15: R1–R11
9. Heller MJ (1996) IEEE Eng Med Biol 100–104
10. Kelley SO, Boon EM, Barton JK, Jackson NM, Hill MG (1999) Nucleic Acids Res 27:4830–4837
11. Borgmann S, Hartwich G, Schulte A, Schuhmann W (2005) Amperometric enzyme sensors based on direct and mediated electron transfer perspectives. In: Palecek E, Scheller F, Wang J (eds) Bioanalysis, vol 1. Electrochemistry of nucleic acids and proteins. Towards electrochemical sensors for genomics and proteomics. Elsevier, Amsterdam
12. Berney H, West J, Haefele E, Alderman J, Lane W, Collins JK (2000) Sens Actuat B 58:100–108
13. Yu CJ, Wan Y, Yowanto H, Li J Tao C, James MD, Tan CL, Blackburn GF, Meade TJ (2001) J Am Chem Soc 123:11155–11161
14. Nakayama M, Ihara T, Nakano K, Maeda M (2002) Talanta 56:857–866
15. Turcu F, Schulte A, Hartwich G, Schuhmann W (2004) Biosens Bioelectron 20:925–932
16. Marques LPJ, Cavaco I, Pinheiro JP, Ferreira VR, Ferreira GNM (2203) Clin Chem Lab Med 41:475–481
17. Schena M (2000) Microarray biochip technology. Eaton, Natick
18. Lockhart DJ, Dong H, Byrne MC, Follettie MT, Gallo MV, Chee MS (1996) Bio/Technology 14:1675–1680
19. Livache T, Fouque B, Roget A, Marchand J, Bidan G, Téoule R, Mathis G (1998) Anal Biochem 255:188–194
20. Dhiman N, Bonilla R, O'KAne D, Poland GA (2002) Vaccine 20:22–30
21. Neugebauer S, Müller U, Lohmüller T, Spatz JP, Stelzle M, Schuhmann W (2006) Electroanalysis 18:1929–1936
22. Schienle M, Paulus C, Frey A, Hofmann F, Holzapfl B, Schindler-Bauer P, Thewes R (2004) IEEE J Solid-State Circuits 39 (12):2438–2445
23. Chen RJ, Bangsaruntip S, Drouvalakis KA, Kam NWS, Shim M, Li Y (2003) Proc Natl Acad Sci USA 100:4984–4989
24. Li Z, Chen Y, Li X, Kamins TI, Nauka K, Williams RS (2004) Nanoletters 4:245–247
25. Rand DAJ, Woods R (1971) J Electroanal Chem Interfacial Electrochem 31:29–38
26. Hartwich G (2007) Patent application DE 2007 044 664
27. Gait MJ (1984) Oligonucleotide synthesis: a practical approach. IRL, Oxford
28. Pon RT, Yu S, Sanghvi YS (1999) Bioconjugate Chem 10:1051–1057
29. Aylward GH, Findlay TJV (1986) Datensammlung Chemie in SI-Einheiten. Wiley-VCH, Weinheim
30. Buckingham DA, Dwyer FP, Goodwin HA, Sargeson AM (1964) Aust J Chem 17:315–324
31. Gallagher SR, Desjardins PR (2006) Curr Protoc Mol Biol App 3: Appendix 3D
32. Bard AJ, Faulkner LR (2001) Electrochemical methods: fundamentals and applications, 2nd ed. Wiley, New York
33. The 5-V DC 96-fold multiplexer on the basis of a relay switching output is addressed by a 7-bit signal at 4-ms operation time and almost no leaking current
34. MP-32 is a USB 2-compatible 12-V DC potentistat with ± 2-V voltage range (@ 16-bit DAC and 7.5-kHz sampling frequency) and a current range of ± 65 nA (@ 16-bit ADC and 50-kHz sampling frequency), current noise is <10 pA
35. The 12-V DC USB 2.0-compatible TCX temperature element consists of a PI-controller with 20-W heating output, a maximum heating rate of 15 °C/min. Temperature accuracy is <± 0.1 °C
36. Haker U, Hartwich G, Frischmann P, Wieder H (2001) Patent DE 101 41 691
37. Dubois LH, Zegarski BR, Nuzzo RG (1987) PNAS 84:4739–4742
38. Li Z, Jin RC, Mirkin CA, Letsinger RL (2002) Nucleic Acids Res 30:1558–1562
39. Demers LM, Mirkin CA, Mucic RC, Reynolds RA, Letsinger RL, Elghanian R, Viswanadham G (2000) Anal Chem 72:5535–5541
40. Letsinger RL, Elghanian R, Viswanadham G, Mirkin CA (2000) Bioconjug Chem 11:289–291
41. A speculative rational for this kind of posttreatment may be that undecanthiol in EtOH causes the capture probes to collapse, leaving the direct vicinity of the capture probe unmodified; these areas can subsequently be modified by hexanthiol in aqueous buffer, where the capture probes supposedly adopts a stretched conformation
42. Herne TM, Tarlov MJ (1997) J Am Chem Soc 119:8916–8920
43. Peterlinz KA, Georgiadis RM, Herne TM, Tarlov MJ (1997) J Am Chem Soc 119:3401–3402
44. Steel AB, Herne TM, Tarlov MJ (1998) Anal Chem 70:4670–4677
45. Steel AB, Levicky RL, Herne TM, Tarlov MJ (2000) Biophys J 79(2):975–981
46. Rekesh D, Lyubchenko L, Shlyakhtenko L, Lindsay SM (1996) Biophys J 71(2):1079–1086
47. O'Connor SD, Olsen GT, Creager SE (1999) J Electroanal Chem 463:197–202
48. Wieder H, Hillebrandt H, Hartwich G et al. (to be published)
49. Bosch FX, Manos MM, Munoz N, Sherman M, Jansen AM, Peto J, Schiffman MH, Moreno V, Kurman R, Shah KV (1995) J Natl Cancer Inst 87:796–802
50. Remmink AJ, Walboomers JMM, Helmerhorts TJM, Voorhorts FJ, Roozendaal L, Risse EKJ, Meijer CJLM, Kenemans P (1995) Int J Cancer 61:306–311
51. Sensitivity and selectivity of the sensors are not influenced by this spread of initial signals (data not shown)
52. A preliminary comparative analysis of the PCR performance by quantitative PCR (procedure analogous to the one described in: Swillens S, Goffard JC, Maréchal Y, Alban de Kerchove d'Exaerde A, Hakim El Housni H (2004) Nucleic Acids Res 32: e56 ) showed that the PCR was started at about 1,000 copies of the sequence that was monitored by EDDA